Optimal Control of Large Space Structures Using Distributed Gyricity

C. J. Damaren* and G. M. T. D'Eleuterio†
University of Toronto, Downsview, Ontario, Canada

An optimal formulation is developed for the shape control of large flexible spacecraft possessing a distribution of control moment gyros. The structure is modeled as a continuum in mass, stiffness, and gyricity (stored angular momentum). A small, linear viscous damping term completes the dynamical description. The equation of motion is formulated in continuum form, and a brief eigenanalysis is presented that permits the modal equations of motion to be derived. The optimal control problem is treated using distributed-parameter concepts, and a modal expansion for the resulting Riccati operator reduces the problem to the solution of a matrix Riccati equation. Such an approach permits pointwise control moment gyros as well as the distributed analog to be handled with the same theory. By means of an example, the use of distributed gyricity is demonstrated to be very effective for shape control of large space structures. Moreover, the notion of a continuous distribution of gyricity is shown to be beneficial in modeling the dynamics and control of flexible spacecraft employing many control moment gyros.

I. Introduction

THE concept of a "gyroelastic" continuum has recently been advanced[1-4] as a model for structures that, in addition to being characterized by a continuous distribution of mass and stiffness, contain a continuous distribution of gyricity (stored angular momentum). This model is a very convenient, useful representation of elastic structures with a large number of small spinning rotors. In fact, the principal motivation here derives from the advent of large, flexible space structures where momentum wheels or control moment gyros may be employed for attitude and shape control.

The use of angular-momentum-exchange devices in the control of flexible spacecraft offers an attractive option. Such devices can provide a control-torque distribution to complement control forces supplied by thrusters. But, unlike thrusters, they are clean actuators and require no refueling and relatively little maintenance. It is significant that the NASA Langley Research Center has established a flexible-grid laboratory facility[5] that has involved the use of reaction wheels for control experiments.[6]

In this paper, we present an optimal formulation for the shape control of flexible spacecraft using "gyric" actuators. It should be clarified that "optimality" in this case may take on two meanings. One can speak of an optimal gyricity distribution or an optimal control law for a given gyricity distribution. It is the latter that we will address by considering a flexible spacecraft with a distribution of control moment gyros.

The optimal control problem is formulated in continuum terms. The continuum approach appears to be experiencing a renaissance in control theory. It permits us, for example, to generalize to distributed (continuous) actuators. However, although the continuum approach may be advantageous for analytical purposes, discretization is ultimately required for computer implementation. To this end, a discretization procedure for the continuum Riccati equation is introduced for systems with rigid modes. In addition, it is shown that, under certain conditions (i.e., the diagonal dominance of a certain matrix), the system matrix Riccati equation reduces to a set of 2×2 matrix Riccati equations.

However, we shall first briefly review the dynamics of gyroelastic systems and then extend the analysis to include light damping. A numerical example demonstrating some of the theoretical results will also be presented.

II. Lightly Damped Gyroelastic Vehicles

Consider the gyroelastic vehicle V depicted in Fig. 1. It consists of a number of flexible appendages, collectively denoted by E, attached to a rigid body R. An origin O is affixed to the rigid body (which, without loss in generality, can be made arbitrarily small). The vehicle is imbued with a distribution of gyricity denoted by $\boldsymbol{h}_s(\boldsymbol{r})$. For now, we restrict $\boldsymbol{h}_s(\boldsymbol{r})$ to be constant with respect to a local reference frame at $\boldsymbol{r}$.

The total displacement of the vehicle may be expressed as

$$\boldsymbol{w}(\boldsymbol{r},t) = \boldsymbol{w}_0(t) - \boldsymbol{r}^{\times}\boldsymbol{\theta}(t) + \begin{cases} \boldsymbol{u}_e(\boldsymbol{r},t), & \boldsymbol{r}\in E \\ \boldsymbol{0}, & \boldsymbol{r}\in R \end{cases} \tag{1}$$

where $\boldsymbol{w}_0$ is the translation of O, $\boldsymbol{\theta}$ is the small rotation of R relative to inertial space, and $\boldsymbol{u}_e(\boldsymbol{r},t)$ is the small deformation of E relative to R. It has been shown[2-4] that the equation of motion for V is

$$\mathscr{M}\ddot{\boldsymbol{w}} + \mathscr{G}\dot{\boldsymbol{w}} + \mathscr{K}\boldsymbol{u}_e = \boldsymbol{f}_{eT}(\boldsymbol{r},t) \tag{2}$$

where $\boldsymbol{f}_{eT}$ represents the external force/volume distribution.

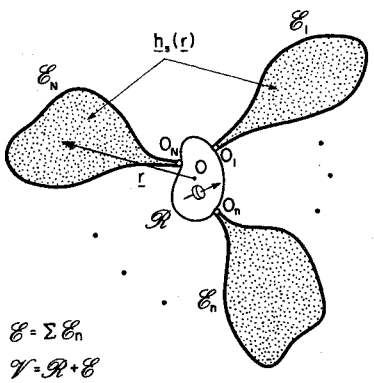

Fig. 1 A gyroelastic vehicle.

Paper presented at the Sixth VPI&SU/AIAA Symposium on Dynamics and Control of Large Structures, Blacksburg, VA, June 29-July 1, 1987; received Feb. 26, 1988; revision received June 16, 1988.

*Doctoral Candidate, Institute for Aerospace Studies.
†Assistant Professor and NSERC University Research Fellow, Institute for Aerospace Studies.

The stiffness operator $\mathscr{K}$, usually differential in form, is self-adjoint

$$\int_V w_1^T \mathscr{K} w_2 \, dV = \int_V w_2^T \mathscr{K} w_1 \, dV \tag{3}$$

Moreover, since V is unconstrained, $\mathscr{K}$ is positive-semidefinite with respect to w:

$$\int_V w^T \mathscr{K} w \, dV \geq 0 \tag{4}$$

The rigid degrees of freedom, which together may be expressed as

$$\mathbf{U}_r = [\mathbf{1} \; -r^\times] \tag{5}$$

in fact span the null space of $\mathscr{K}$, i.e.,

$$\mathscr{K}\mathbf{U}_r = \mathbf{O}$$

It is important to observe that $\mathscr{K}$, although only positive-semidefinite with respect to w, is positive-definite with respect to u_e, i.e.,

$$\int_E u_e^T \mathscr{K} u_e \, dV > 0, \qquad u_e \not\equiv \mathbf{0} \tag{6}$$

The mass operator $\mathscr{M}$ is defined simply as $\sigma(r)\mathbf{1}$ where $\sigma(r)$ is the mass density and $\mathbf{1}$ represents the identity operator. Clearly, $\mathscr{M}$ is self-adjoint and positive-definite (with respect to w). Finally, and of central interest here,

$$\mathscr{G} \triangleq -\tfrac{1}{4}\nabla^\times h_s{}^\times \nabla^\times \tag{7}$$

is the skew-adjoint gyricity operator. (For convenience, h_s is assumed to vanish on ∂V, the boundary of V.)

It should be mentioned, and indeed emphasized, that the assumption that $h_s(r)$ is continuous does not limit our analysis in any way. To model lumped sources of stored angular momentum, we can employ Dirac's delta function as follows:

$$h_s(r) = \sum_{i=1}^{n} h_i \, \delta(r - r_i) \tag{8}$$

We shall implement this form in part of the numerical example.

The equation of motion (2) omits the effect of structural damping. But, given its importance in dynamics and control, damping cannot, in practice, be ignored. Thus, let the dissipative influences be modeled as

$$f_D = -\mathscr{D}\dot{w} \tag{9}$$

where the damping operator is linear and time-invariant. Also, $\mathscr{D}$ is self-adjoint and possesses the same null-space as $\mathscr{K}$, rendering it positive-semidefinite with respect to w. However, we shall assume complete damping, hence

$$\int_E \dot{u}_e^T \mathscr{D} \dot{u}_e \, dV > 0, \qquad \dot{u}_e \not\equiv \mathbf{0} \tag{10}$$

Furthermore, large space structures are typically lightly damped, which implies that

$$\int_0^T \|\mathscr{D}\dot{w}\| \, dt \ll \int_0^T \|\mathscr{K} u_e\| \, dt \tag{11}$$

i.e., the dissipative forces are much smaller than the stiffness forces. It should be acknowledged that many elaborate models for damping exist. Equation (9) represents a relatively simple viscous damping model, yet it is quite useful and very instructive.

Amending Eq. (2), therefore, to include structural damping yields

$$\mathscr{M}\ddot{w} + (\mathscr{G} + \mathscr{D})\dot{w} + \mathscr{K} u_e = f_{eT} \tag{12}$$

This, then, is the equation of motion for lightly damped gyroelastic vehicles.

III. Modal Analysis

It will prove indispensible to express the equation of motion (12) in first-order form:

$$\mathscr{E}\dot{\chi} + \mathscr{T}\chi = \mathbf{f}_{eT} \tag{13}$$

where

$$\mathscr{E} = \begin{bmatrix} \mathscr{M} & \cdot \\ \cdot & \mathscr{K} \end{bmatrix} \quad \mathscr{T} = \begin{bmatrix} \mathscr{G} + \mathscr{D} & \mathscr{K} \\ -\mathscr{K} & \cdot \end{bmatrix} \quad \chi = \begin{bmatrix} \dot{w} \\ u_e \end{bmatrix} \mathbf{f}_{eT} = \begin{bmatrix} f_{eT} \\ \cdot \end{bmatrix}$$

At this juncture, let us introduce the following inner product:

$$\langle \phi, \psi \rangle \triangleq \int_V \phi^T \psi \, dV \tag{14}$$

The operator $\mathscr{E}$ is self-adjoint, which, in the notation of this inner product, means

$$\langle \chi_1, \mathscr{E}\chi_2 \rangle = \langle \mathscr{E}\chi_1, \chi_2 \rangle \tag{15}$$

for χ_1 and χ_2 satisfying the boundary conditions. In addition, owing to our choice of the state description χ, $\mathscr{E}$ is positive-definite, i.e.,

$$\langle \chi, \mathscr{E}\chi \rangle > 0 \quad (\chi \not\equiv 0) \tag{16}$$

The operator $\mathscr{T}$ can be decomposed into skew-adjoint and self-adjoint parts:

$$\mathscr{T} = \mathscr{S} + \delta\mathscr{S} \tag{17}$$

where

$$\mathscr{S} \triangleq \begin{bmatrix} \mathscr{G} & \mathscr{K} \\ -\mathscr{K} & \cdot \end{bmatrix}, \qquad \delta\mathscr{S} \triangleq \begin{bmatrix} \mathscr{D} & \cdot \\ \cdot & \cdot \end{bmatrix}$$

and

$$\langle \chi_1, \mathscr{S}\chi_2 \rangle = -\langle \mathscr{S}\chi_1, \chi_2 \rangle, \qquad \langle \chi_1, \delta\mathscr{S}\chi_2 \rangle = \langle \delta\mathscr{S}\chi_1, \chi_2 \rangle$$

The adjoint of $\mathscr{T}$ defined such that

$$\langle \mathscr{T}^*\chi_1, \chi_2 \rangle = \langle \chi_1, \mathscr{T}\chi_2 \rangle \tag{18}$$

is

$$\mathscr{T}^* = -\mathscr{S} + \delta\mathscr{S} \tag{19}$$

Note that, in view of the light damping assumption, we are treating damping as a perturbation to the reference (undamped) gyroelastic system.

In preparation for an eigenanalysis of Eq. (13), we shall briefly review the eigenproblem for the undamped case,[2,3] which is

$$\lambda_\alpha \mathscr{E}\chi_\alpha + \mathscr{S}\chi_\alpha = \mathbf{0} \tag{20}$$

The properties of $\mathscr{E}$ and $\mathscr{S}$ dictate that λ_α and χ_α appear in complex-conjugate pairs and that λ_α are purely imaginary. We can therefore write

$$\lambda_\alpha = j\omega_\alpha, \qquad \chi_\alpha = \phi_\alpha + j\psi_\alpha, \qquad (\alpha = -\infty, \ldots, \infty) \tag{21}$$

where $\omega_{-\alpha} = -\omega_\alpha, \omega_\alpha > 0$ for $\alpha > 0$, and $\boldsymbol{\phi}_{-\alpha} = \boldsymbol{\psi}_\alpha$. (Note that 0 is excluded from the range of α.) The real eigenfunctions $\boldsymbol{\phi}_\alpha$ and $\boldsymbol{\psi}_\alpha$ have the form

$$\boldsymbol{\phi}_\alpha = \begin{bmatrix} -\omega_\alpha \boldsymbol{v}_\alpha \\ \boldsymbol{u}_{e\alpha} \end{bmatrix}, \qquad \boldsymbol{\psi}_\alpha = \begin{bmatrix} \omega_\alpha \boldsymbol{u}_\alpha \\ \boldsymbol{v}_{e\alpha} \end{bmatrix} \tag{22}$$

where $\boldsymbol{u}_{-\alpha} = \boldsymbol{v}_\alpha$ and $\boldsymbol{u}_{e,-\alpha} = \boldsymbol{v}_{e\alpha}$.

As the system is unconstrained, there are also zero-frequency eigenfunctions:

$$\lambda = 0, \qquad \mathscr{S}\mathbf{X}_r = \mathbf{O} \tag{23}$$

If we partition $\mathbf{X}_r$ as

$$\mathbf{X}_r = \begin{bmatrix} \mathbf{U}_r \\ \mathbf{U}_e \end{bmatrix} \tag{24}$$

the corresponding modes are defined by $\mathscr{K}\mathbf{U}_r = \mathbf{O}$, $\mathscr{G}\mathbf{U}_r + \mathscr{K}\mathbf{U}_e = \mathbf{O}$. In the case of a purely elastic body ($\mathscr{G} = \mathbf{O}$), these modes are simply the rigid (position) modes ($\mathbf{U}_r = \mathbf{U}_r, \mathbf{U}_e = \mathbf{O}$). In the gyroelastic case, $\mathbf{X}_r$ has the form

$$\mathbf{X}_r = \begin{bmatrix} \mathbf{1} & -\boldsymbol{r}^\times \boldsymbol{a} \\ \cdot & \boldsymbol{u}_a \end{bmatrix} \tag{25}$$

The first "column" represents the translational modes, which are unaffected by gyricity, whereas the second consists of the "pseudorigid modes," which may be described as uniform rotations about an axis $\boldsymbol{a}$ with the elastic appendages of the vehicle in a constant deformed state $\boldsymbol{u}_a(\boldsymbol{r})$.[4] We shall refer to $\mathbf{X}_r$ as the rigid rate modes.

The orthonormality relationships among the eigenfunctions can be summarized as follows:

$$\langle \boldsymbol{\phi}_\alpha, \mathscr{E}\boldsymbol{\phi}_\beta \rangle = 2\omega_\alpha^2 \delta_{\alpha\beta}, \qquad \langle \boldsymbol{\phi}_\alpha, \mathscr{E}\mathbf{X}_r \rangle = \mathbf{0}, \quad \langle \mathbf{X}_r, \mathscr{E}\mathbf{X}_r \rangle \triangleq \mathbf{M}_r > \mathbf{O} \tag{26a}$$

$$\langle \boldsymbol{\psi}_\alpha, \mathscr{S}\boldsymbol{\phi}_\beta \rangle = 2\omega_\alpha^3 \delta_{\alpha\beta} \tag{26b}$$

By virtue of Eq. (23), $\boldsymbol{\phi}_\alpha$ are also orthogonal to $\mathbf{X}_r$ with respect to $\mathscr{S}$.

The presence of light damping results in perturbations in both the eigenvalues and the eigenfunctions. A detailed perturbation analysis has been performed[7]; however, only a brief overview will have to suffice here. The eigenproblem associated with the damped equation of motion (13) is

$$\lambda'_\alpha \mathscr{E}\boldsymbol{\chi}'_\alpha + \mathscr{T}\boldsymbol{\chi}'_\alpha = \mathbf{0} \tag{27}$$

where

$$\lambda'_\alpha = \lambda_\alpha + \delta\lambda_\alpha, \qquad \boldsymbol{\chi}'_\alpha = \boldsymbol{\chi}_\alpha + \delta\boldsymbol{\chi}_\alpha$$

Since the operator $\mathscr{T}$ is non-self-adjoint, it is also necessary to consider the corresponding adjoint eigenproblem,

$$\lambda'^*_\alpha \mathscr{E}\boldsymbol{\xi}'_\alpha + \mathscr{T}^*\boldsymbol{\xi}'_\alpha = \mathbf{0} \tag{28}$$

where

$$\boldsymbol{\xi}'_\alpha = \boldsymbol{\xi}_\alpha + \delta\boldsymbol{\xi}_\alpha$$

are the (complex) adjoint eigenfunctions with $\boldsymbol{\xi}_\alpha = \boldsymbol{\chi}_\alpha$ (the undamped case).

The damped system eigenvalues are

$$\lambda'_\alpha = -\zeta_\alpha \omega_\alpha + j\omega_\alpha, \qquad \alpha = -\infty, \ldots, \infty \tag{29}$$

where

$$\zeta_\alpha = -\zeta_{-\alpha} \triangleq \frac{1}{4\omega_\alpha} \{ \langle \boldsymbol{u}_{e\alpha}, \mathscr{D}\boldsymbol{u}_{e\alpha} \rangle + \langle \boldsymbol{v}_{e\alpha}, \mathscr{D}\boldsymbol{v}_{e\alpha} \rangle \}$$

are the damping factors. Note that the first-order perturbation is strictly real and, as a result of complete damping, $\zeta_\alpha \omega_\alpha > 0$. The zero-frequency eigenvalues are unaffected by damping as are their corresponding modes.

The perturbations in the eigenfunctions have the form

$$\delta\boldsymbol{\chi}_\alpha = \delta\boldsymbol{\phi}_\alpha + j\delta\boldsymbol{\psi}_\alpha, \qquad \delta\boldsymbol{\xi}_\alpha = -\delta\boldsymbol{\phi}_\alpha - j\delta\boldsymbol{\psi}_\alpha \tag{30}$$

Without loss in generality, we may take $\delta\boldsymbol{\phi}_{-\alpha} = \delta\boldsymbol{\psi}_\alpha$. Furthermore, we can expand $\delta\boldsymbol{\phi}_\alpha$ in terms of the unperturbed eigenfunctions, i.e.,

$$\delta\boldsymbol{\phi}_\alpha = \sum_{\beta=-\infty}^{\infty} c_{\alpha\beta} \boldsymbol{\phi}_\beta \tag{31}$$

where

$$c_{\alpha\beta} = \frac{\omega_\alpha \omega_\beta D_{-\alpha,\beta} - \omega_\alpha^2 D_{\alpha,-\beta}}{2\omega_\beta(\omega_\beta^2 - \omega_\alpha^2)}, \qquad |\alpha| \neq |\beta|$$

$$c_{\alpha\alpha} = -\frac{D_{\alpha,-\alpha}}{4\omega_\alpha}, \qquad c_{\alpha,-\alpha} = \frac{D_{-\alpha,-\alpha} - D_{\alpha,\alpha}}{8\omega_\alpha}$$

and $D_{\alpha\beta} \equiv D_{\beta\alpha} \triangleq \langle \boldsymbol{u}_{e\alpha}, \mathscr{D}\boldsymbol{u}_{e\beta} \rangle$. The coefficients $c_{\alpha\alpha}$ and $c_{\alpha,-\alpha}$ are determined uniquely by considering the orthonormality conditions for the perturbed eigenfunctions.

Denoting the perturbed (real) eigenfunctions and adjoint eigenfunctions by

$$\boldsymbol{\varphi}_\alpha \triangleq \boldsymbol{\phi}_\alpha + \delta\boldsymbol{\phi}_\alpha, \qquad \boldsymbol{\vartheta}_\alpha \triangleq \boldsymbol{\phi}_\alpha - \delta\boldsymbol{\phi}_\alpha \tag{32}$$

we find that the following biorthogonality relations hold:

$$\langle \boldsymbol{\vartheta}_\alpha, \mathscr{E}\boldsymbol{\varphi}_\beta \rangle = 2\omega_\alpha^2 \delta_{\alpha\beta}, \qquad \langle \boldsymbol{\vartheta}_\alpha, \mathscr{T}\boldsymbol{\varphi}_\beta \rangle = 2\omega_\alpha^3 (\zeta_\alpha \delta_{\alpha\beta} - \delta_{-\alpha,\beta}) \tag{33}$$

In addition,

$$\langle \boldsymbol{\vartheta}_\alpha, \mathscr{E}\mathbf{X}_r \rangle = \langle \boldsymbol{\varphi}_\alpha, \mathscr{E}\mathbf{X}_r \rangle = \langle \boldsymbol{\vartheta}_\alpha, \mathscr{T}\mathbf{X}_r \rangle = \langle \boldsymbol{\varphi}_\alpha, \mathscr{T}\mathbf{X}_r \rangle = \mathbf{0} \tag{34}$$

The preceding results may be compared to those of Meirovitch and Ryland[8] for discretized systems. It should be pointed out, however, that unlike the latter-mentioned results, where quantities corresponding to $c_{\alpha\alpha}$ and $c_{\alpha,-\alpha}$ are arbitrarily set to zero, the present results are consistent with the recent cautionary remarks of Lim et al.[9]

The general solution for the motion of our system can be expressed in terms of the rate modes $\mathbf{X}_r$ and the damped (perturbed) eigenfunctions $\boldsymbol{\varphi}_\alpha$:

$$\boldsymbol{\chi}(\boldsymbol{r},t) = \mathbf{X}_r(\boldsymbol{r})\boldsymbol{\eta}_r(t) + \sum_{\beta=-\infty}^{\infty} \boldsymbol{\varphi}_\beta(\boldsymbol{r})\eta_\beta(t) \tag{35}$$

Substituting into Eq. (13) and operating with $\langle \mathbf{X}_r, \cdot \rangle$ and $\langle \boldsymbol{\vartheta}_\alpha, \cdot \rangle$, while observing the orthogonality conditions, we arrive at the modal equations of motion

$$\mathbf{M}_r \ddot{\boldsymbol{\eta}}_r = \mathbf{f}_r$$

$$\dot{\eta}_\alpha + \zeta_\alpha \omega_\alpha \eta_\alpha - \omega_\alpha \eta_{-\alpha} = \frac{1}{2\omega_\alpha}(\zeta_\alpha f_\alpha - f_{-\alpha})$$

$$\alpha = 1, \ldots, \infty \tag{36}$$

$$\dot{\eta}_{-\alpha} + \omega_\alpha \eta_\alpha + \zeta_\alpha \omega_\alpha \eta_{-\alpha} = \frac{1}{2\omega_\alpha}(f_\alpha + \zeta_\alpha f_{-\alpha})$$

where

$$\mathbf{f}_r \triangleq \int_V \mathbf{U}_r^T \boldsymbol{f}_{eT}\, dV, \qquad f_\alpha \triangleq \int_V \boldsymbol{\mu}_\alpha^T \boldsymbol{f}_{eT}\, dV$$

and $\boldsymbol{\mu}_\alpha \triangleq \boldsymbol{u}_\alpha - \delta\boldsymbol{u}_\alpha$ are the perturbed adjoint-mode shapes

available from ϑ_α:

$$\vartheta_\alpha = \begin{bmatrix} -\omega_\alpha \mu_{-\alpha} + \zeta_\alpha \omega_\alpha \mu_\alpha \\ \mu_{e\alpha} \end{bmatrix}$$

The equations for the elastic model coordinates can be conveniently written as

$$\dot{\eta}_e + \Omega \eta_e = \tfrac{1}{2}\Omega^{-T} \mathbf{f}_e \tag{37}$$

where

$$\eta_e \triangleq \text{col}\{\eta_\alpha, \eta_{-\alpha}\}, \quad \Omega \triangleq \text{diag}\left\{\omega_\alpha \begin{bmatrix} \zeta_\alpha & -1 \\ 1 & \zeta_\alpha \end{bmatrix}\right\}, \quad \mathbf{f}_e \triangleq \text{col}\{f_\alpha, f_{-\alpha}\}$$

Note the bicoupled form of the elastic modal equations.

A few words are perhaps in order regarding the foregoing perturbation analysis. As is evident, light damping has only a first-order effect on the eigenvalues and eigenfunctions. However, the perturbation in the eigenfunctions is qualitatively insignificant compared with the effect on the eigenvalues. The modal character of a system is barely influenced by a 1% change, say, in the mode shapes, but a 1% damping factor has major effects, namely, the exponential decay of unforced responses and finite responses to resonant forces. Therefore, it can be argued that, for lightly damped systems, it is sufficient to consider only the first-order perturbations in the eigenvalues and assume the eigenfunctions are essentially unchanged. (See also, for example, the discussion by Hughes.[10]) The practical consequences of this argument are important, since the damping factors are usually estimated directly without having to identify explicitly the damping operator $\mathscr{D}$ or its matrix counterpart in the discretized case. This fact will be exploited in the numerical example.

IV. Optimal Control Formulation

Let us now focus our attention on the use of gyricity in active control. A spinning rotor can be employed as control-torque actuator by regulating either the magnitude of the rotor's angular momentum or the angular rate of the rotor's spin axis. The former method is used by momentum wheels and the latter by control moment gyros. We shall consider a distribution of control moment gyros only and the (time-varying) gyricity therefrom.

We associate with the (nominal) gyricity distribution $\boldsymbol{h}_s(\boldsymbol{r})$, a distribution of gimbal angles

$$\boldsymbol{\beta}(\boldsymbol{r},t) \triangleq \text{col}\{\beta_x, \beta_y, \beta_z\} \tag{38}$$

which is assumed small, i.e.,

$$\|\boldsymbol{\beta}\| \ll 1 \tag{39}$$

The column of angles $\boldsymbol{\beta}(\boldsymbol{r},t)$ represents the angular displacement of the gyricity element $\boldsymbol{h}_s(\boldsymbol{r})\,\mathrm{d}V$ with respect to the local reference frame at $\boldsymbol{r}$. As expressed in this frame, the gyricity distribution is

$$\boldsymbol{h}_\beta(\boldsymbol{r},t) = [\mathbf{1} + \boldsymbol{\beta}^\times(\boldsymbol{r},t)]\boldsymbol{h}_s(\boldsymbol{r})$$

The torque distribution arising from $\boldsymbol{h}_\beta$ is given by

$$\boldsymbol{g}_h(\boldsymbol{r},t) = -[\dot{\boldsymbol{h}}_\beta + \dot{\boldsymbol{\alpha}}^\times(\boldsymbol{r},t)\boldsymbol{h}_\beta] \tag{40}$$

where $\boldsymbol{\alpha} = \frac{1}{2}\nabla^\times \boldsymbol{w}$ is the total (rigid plus elastic) rotational displacement at $\boldsymbol{r}$. Hence, the equivalent force distribution acting on the vehicle is[1]

$$\boldsymbol{f}_h(\boldsymbol{r},t) = \tfrac{1}{2}\nabla^\times \boldsymbol{g}_h(\boldsymbol{r},t) = -\mathscr{G}\dot{\boldsymbol{w}} + \mathscr{H}\boldsymbol{v} \tag{41}$$

where we recognize the first term from Eq. (12) and

$$\mathscr{H} \triangleq \tfrac{1}{2}\nabla^\times \boldsymbol{h}_s^\times, \qquad \boldsymbol{v} \triangleq \dot{\boldsymbol{\beta}}$$

We thus identify the (distributed) control force as

$$\boldsymbol{f}_c(\boldsymbol{r},t) = \mathscr{H}\boldsymbol{v} \tag{42}$$

and $\boldsymbol{v}$ as the (distributed) control variable. The ensuing equation of motion is

$$\mathscr{M}\ddot{\boldsymbol{w}} + (\mathscr{G} + \mathscr{D})\dot{\boldsymbol{w}} + \mathscr{K}\boldsymbol{u}_e = \mathscr{H}\boldsymbol{v} + \boldsymbol{f}_d \tag{43}$$

or, in first-order form,

$$\mathscr{E}\dot{\boldsymbol{\chi}} + \mathscr{T}\boldsymbol{\chi} = \mathscr{B}\boldsymbol{v} + \boldsymbol{f}_d \tag{44}$$

where

$$\mathscr{B} \triangleq \begin{bmatrix} \mathscr{H} \\ \cdot \end{bmatrix}, \qquad \boldsymbol{f}_d \triangleq \begin{bmatrix} \boldsymbol{f}_d \\ \cdot \end{bmatrix}$$

and $\boldsymbol{f}_d(\boldsymbol{r},t)$ represents disturbance forces. For future reference, we also mention that

$$\mathscr{B}^* = [\mathscr{H}^* \ \cdot\ ], \qquad \mathscr{H}^* = -\tfrac{1}{2}\boldsymbol{h}_s^\times \nabla^\times$$

are the adjoints of $\mathscr{B}$ and $\mathscr{H}$.

Before the optimal control problem is tackled, a couple of notational issues should be addressed. First, we shall indicate by U the space of all possible controls $\boldsymbol{v}$. For emphasis, then, inner products involving the control variable will be written as

$$\langle \boldsymbol{v}_1, \boldsymbol{v}_2 \rangle_U = \int_V \boldsymbol{v}_1^T \boldsymbol{v}_2 \, \mathrm{d}V$$

We shall also find it convenient to introduce an outer product, corresponding to Eq. (14) and denoted by $\boldsymbol{\phi}\rangle\langle\boldsymbol{\psi}$, which is defined such that

$$[\boldsymbol{\phi}\rangle\langle\boldsymbol{\psi}]\boldsymbol{\chi} \triangleq \boldsymbol{\phi}\langle\boldsymbol{\psi},\boldsymbol{\chi}\rangle$$

and

$$\langle \boldsymbol{\chi}_1, [\boldsymbol{\phi}\rangle\langle\boldsymbol{\psi}]\boldsymbol{\chi}_2 \rangle \triangleq \langle \boldsymbol{\chi}_1, \boldsymbol{\phi}\rangle\langle\boldsymbol{\psi},\boldsymbol{\chi}_2\rangle$$

Of course, the arguments are not limited to column functions but may include matrix functions as well.

Let us define a set of admissible controls as

$$U_{ad} \triangleq \{\boldsymbol{v} \in U \mid \int_0^T \langle \boldsymbol{v},\boldsymbol{v} \rangle_U \, \mathrm{d}t < \infty\} \tag{45}$$

where T is the terminal time of interest. We seek the optimal control $\boldsymbol{v}^\star \in U_{ad}$ such that

$$J(\boldsymbol{v}^\star) \le J(\boldsymbol{v}), \qquad \forall \boldsymbol{v} \in U_{ad}$$

where

$$J(\boldsymbol{v}) = \frac{1}{2}\int_0^T \langle \boldsymbol{\chi}(\boldsymbol{v}), \mathscr{Q}\boldsymbol{\chi}(\boldsymbol{v}) \rangle + \langle \boldsymbol{v}, \mathscr{R}\boldsymbol{v} \rangle_U \, \mathrm{d}t \tag{46}$$

The operator $\mathscr{R}$ is self-adjoint and positive definite. The operator $\mathscr{Q}$ is also self-adjoint but non-negative definite. Both $\mathscr{R}$ and $\mathscr{Q}$, however, are restricted to be time-invariant. We shall assume that the rigid rate modes are not penalized in the cost functional, i.e., $\mathscr{Q}\mathbf{X}_r \equiv \mathbf{O}$, since the translational modes are uncontrollable via the gyricity distribution. (The pseudo-rigid modes could be included without difficulty; however, for explanatory purposes we choose not to penalize them.) As an example, consider

$$\mathscr{Q} = \mathscr{E} - \mathscr{E}\mathbf{X}_r \rangle \mathbf{M}_r^{-1} \langle \mathscr{E}\mathbf{X}_r \tag{47}$$

The term $\langle \chi, \mathcal{Q}\chi \rangle$ thus expresses the total energy (less the "spin" energy due to gyricity) of all the elastic modes of the structure.

If the disturbances are neglected ($f_d \equiv \mathbf{0}$), the solution to the optimal control problem (derived in the Appendix) can be expressed as

$$v(r,t) = -\mathcal{R}^{-1}\mathcal{B}^*\xi(r,t) = -\mathcal{R}^{-1}\mathcal{B}^*\mathcal{P}(t)\mathcal{E}\chi(r,t) \quad (48)$$

where the $(\cdot)^*$ notation is dropped for convenience and ξ is the solution of the following adjoint equation:

$$-\mathcal{E}\dot{\xi} + \mathcal{T}^*\xi = \mathcal{Q}\chi, \qquad \xi(r,T) = \mathbf{0}$$

The eigenproblem (28) can be associated with the preceding equation. In Eq. (48), the adjoint function ξ has been expressed as a function of χ, $\xi(r,t) = \mathcal{P}(t)\mathcal{E}\chi(r,t)$, where $\mathcal{P}$ is the unique positive-semidefinite (self-adjoint) solution of the operator Riccati equation

$$\mathcal{E}\dot{\mathcal{P}}\mathcal{E} = \mathcal{E}\mathcal{P}\mathcal{T} + \mathcal{T}^*\mathcal{P}\mathcal{E} + \mathcal{E}\mathcal{P}\mathcal{B}\mathcal{R}^{-1}\mathcal{B}^*\mathcal{P}\mathcal{E} - \mathcal{Q} \quad (49)$$

with terminal condition $\mathcal{P}(T) = \mathbf{O}$. This equation is rather unwieldly in appearance but a constructive solution procedure is within our grasp. Because $\mathcal{P}$ is a bounded linear operator mapping the space of χ into the space of the adjoint variable ξ (via $\mathcal{E}$), it can be expressed using the system eigenfunctions.[11] Thus, we propose the following representation:

$$\begin{aligned}\mathcal{P} = {} & \mathbf{X}_r\rangle\mathbf{M}_r^{-1}\,\mathbf{P}_{rr}\mathbf{M}_r^{-1}\langle\mathbf{X}_r + \frac{1}{2}\sum_{\alpha=-\infty}^{\infty}\omega_\alpha^{-2}\,\vartheta_\alpha\rangle\mathbf{P}_{\alpha r}\mathbf{M}_r^{-1}\langle\mathbf{X}_r \\ & + \frac{1}{2}\sum_{\beta=-\infty}^{\infty}\omega_\beta^{-2}\mathbf{X}_r\rangle\mathbf{M}_r^{-1}\mathbf{P}_{r\beta}\langle\vartheta_\beta \\ & + \frac{1}{4}\sum_{\alpha,\beta=-\infty}^{\infty}\omega_a^{-2}\,\omega_\beta^{-2}\,P_{\alpha\beta}\vartheta_\alpha\rangle\langle\vartheta_\beta \end{aligned} \quad (50)$$

The undetermined coefficients are given by

$$P_{\alpha\beta}(t) = \langle\varphi_\alpha, \mathcal{E}\mathcal{P}\mathcal{E}\varphi_\beta\rangle, \qquad \mathbf{P}_{rr}(t) = \langle\mathbf{X}_r, \mathcal{E}\mathcal{P}\mathcal{E}\mathbf{X}_r\rangle,$$
$$\mathbf{P}_{\alpha r}(t) = \langle\varphi_\alpha, \mathcal{E}\mathcal{P}\mathcal{E}\mathbf{X}_r\rangle$$

by virtue of the orthonormality relations [Eqs. (33) and (34)]. Since $\boldsymbol{P}$ is self-adjoint,

$$P_{\alpha\beta} = P_{\beta\alpha}, \quad \mathbf{P}_{rr} = \mathbf{P}_{rr}^T, \qquad \mathbf{P}_{\alpha r} = \mathbf{P}_{r\alpha}^T$$

If we use the above expression for $\mathcal{P}$ and the modal expansion for χ [Eq. (35)], the adjoint variable $\xi = \mathcal{P}\mathcal{E}\chi$ becomes

$$\begin{aligned}\xi = {} & \mathbf{X}_r\mathbf{M}_r^{-1}\left[\mathbf{P}_{rr}\eta_r + \sum_{\beta=-\infty}^{\infty}\mathbf{P}_{r\beta}\eta_\beta\right] \\ & + \sum_{\alpha=-\infty}^{\infty}\frac{1}{2}\omega_\alpha^{-2}\,\vartheta_\alpha\left[\mathbf{P}_{\alpha r}\eta_r + \sum_{\beta=-\infty}^{\infty}P_{\alpha\beta}\eta_\beta\right]\end{aligned}$$

This is a modal expansion for ξ in terms of $\mathbf{X}_r$ and the adjoint eigenfunctions ϑ_α with the expansion coefficients expressed as linear combinations of the modal coordinates η_r, η_α. Hence, Eq. (50) implements the distributed parameter analog of the usual "sweep method," i.e., a mapping from the state variable to the adjoint variable.

Substituting Eq. (50) into Eq. (49) and successively performing the operations $\langle\mathbf{X}_r, (\cdot)\mathbf{X}_r\rangle$, $\langle\varphi_\alpha, (\cdot)\mathbf{X}_r\rangle$, and $\langle\varphi_\alpha, (\cdot)\varphi_\beta\rangle$ on both sides of the equality, we can obtain the Riccati equations for the coefficients $\mathbf{P}_{rr}$, $\mathbf{P}_{\alpha r}$, and $P_{\alpha\beta}$. Since $\langle\mathbf{X}_r, \mathcal{Q}\mathbf{X}_r\rangle \equiv \mathbf{O}$ and $\langle\mathbf{X}_r, \mathcal{Q}\varphi_\alpha\rangle \equiv \mathbf{0}$, these equations reveal that

$$\mathbf{P}_{rr} \equiv \mathbf{O}, \qquad \mathbf{P}_{\alpha r} \equiv \mathbf{0}, \qquad \alpha = -\infty,\ldots,\infty \quad (51)$$

and

$$\begin{aligned}\dot{P}_{\alpha\beta} = {} & P_{\alpha,-\beta}\omega_\beta + P_{-\alpha,\beta}\omega_\alpha + P_{\alpha\beta}(\zeta_\alpha\omega_\alpha + \zeta_\beta\omega_\beta) \\ & + \frac{1}{4}\sum_{i,j=-\infty}^{\infty}\frac{P_{\alpha i}P_{\beta j}}{\omega_i^2\omega_j^2}\langle\vartheta_i, \mathcal{B}\mathcal{R}^{-1}\mathcal{B}^*\vartheta_j\rangle \\ & - \langle\varphi_\alpha, \mathcal{Q}\varphi_\beta\rangle, \qquad \alpha,\beta = -\infty,\ldots,\infty\end{aligned} \quad (52)$$

subject to $P_{\alpha\beta}(T) = 0$. The discretized Riccati equation (52) can be expressed in a more palatable form by defining

$$\mathbf{P} \triangleq \text{matrix}\{P_{\alpha\beta}\}, \qquad \mathbf{W} \triangleq \text{matrix}\{W_{\alpha\beta}\}, \qquad \mathbf{Q} \triangleq \text{matrix}\{Q_{\alpha\beta}\}$$

where

$$W_{\alpha\beta} \triangleq \int_V \mu_\alpha^T\mathcal{H}\mathcal{R}^{-1}\mathcal{H}^*\mu_\beta\,dV, \qquad Q_{\alpha\beta} \triangleq \int_V \varphi_\alpha^T\mathcal{Q}\varphi_\beta\,dV$$

The matrices $\mathbf{P}$, $\mathbf{W}$, and $\mathbf{Q}$ are symmetric and non-negative-definite because of the corresponding operator properties. With these in hand, the Fourier coefficients $P_{\alpha\beta}$ satisfy a matrix Riccati equation:

$$\dot{\mathbf{P}} = \mathbf{P}\boldsymbol{\Omega} + \boldsymbol{\Omega}^T\mathbf{P} + \tfrac{1}{4}\mathbf{P}\boldsymbol{\Omega}^{-T}\mathbf{W}\boldsymbol{\Omega}^{-1}\mathbf{P} - \mathbf{Q}, \qquad \mathbf{P}(T) = \mathbf{O} \quad (53)$$

where $\boldsymbol{\Omega}$ was defined in Eq. (37). The form of the preceding equation is consistent with the modal description of the state [Eq. (37)].

The optimal control law (48) can be expressed as a function of the modal coordinates η_e. Substituting the expansions for $\mathcal{P}$ [Eq. (50)] and χ [Eq. (35)] into Eq. (48) results in

$$v(r,t) = -\tfrac{1}{2}\boldsymbol{R}^{-1}\mathbf{B}^T(r)\boldsymbol{\Omega}^{-1}\mathbf{P}\eta_e(t) \quad (54)$$

where

$$\mathbf{B}^T(r) \triangleq \text{row}\{\mathcal{H}^*\mu_\alpha, \mathcal{H}^*\mu_{-\alpha}\}$$

The continuum form of the closed-loop motion equation is

$$\mathcal{E}\dot{\chi} + (\mathcal{T} + \mathcal{B}\mathcal{R}^{-1}\mathcal{B}^*\mathcal{P}\mathcal{E})\chi = \mathbf{f}_d$$

and the resulting closed-loop modal equations of motion become

$$\begin{aligned}\mathbf{M}_r\dot{\eta}_r + \tfrac{1}{2}\mathbf{W}_{re}\boldsymbol{\Omega}^{-1}\mathbf{P}\eta_e &= \mathbf{f}_{r,d} \\ \dot{\eta}_e + (\boldsymbol{\Omega} + \tfrac{1}{4}\boldsymbol{\Omega}^{-T}\mathbf{W}\boldsymbol{\Omega}^{-1}\mathbf{P})\eta_e &= \frac{1}{2}\boldsymbol{\Omega}^{-T}\mathbf{f}_{e,d}\end{aligned} \quad (55)$$

where

$$\mathbf{W}_{re} \triangleq \text{row}\{W_{r\alpha}\}, \qquad W_{r\alpha} \triangleq \int_V \mathbf{U}_r^T\mathcal{H}\mathcal{R}^{-1}\mathcal{H}^*\mu_\alpha\,dV$$

and $\mathbf{f}_{r,d}$ and $\mathbf{f}_{e,d}$ are the rigid and elastic modal disturbance forces. The optimal value of the performance index as derived in the Appendix, in continuum form, is

$$J(v^*) = \tfrac{1}{2}\langle\chi(r,0), \mathcal{E}\mathcal{P}(0)\mathcal{E}\chi(r,0)\rangle$$

The eigenfunction expansions for $\mathcal{P}$ and χ provide the matrix representation

$$J(v^*) = \tfrac{1}{2}\eta_e^T(0)\mathbf{P}(0)\eta_e(0)$$

which is analogous to the standard lumped-parameter result.

It is worthwhile to pause for a moment and study the implications of the foregoing equations for pointwise gyric actuators. The control force can still be written as in Eq. (43),

Table 1 Open- and closed-loop eigenvalues

Open-loop frequencies, $\hat{\omega}_\alpha$			Closed-loop eigenvalues, $\hat{\lambda}_\alpha$ Continuous, h_s				Pointwise, $\tilde{h}_s$	
Elastic	Gyroelastic, $\hat{h}_T = 1$		Full $\bar{\mathbf{P}}$		Block diag. $\bar{\mathbf{P}}$		Full $\bar{\mathbf{P}}$	
$\hat{h}_T = 0$	h_s	$\tilde{h}_s$	$\zeta_{d\alpha}$	$\hat{\omega}_{d\alpha}$	$\zeta_{d\alpha}$	$\hat{\omega}_{d\alpha}$	$\zeta_{d\alpha}$	$\hat{\omega}_{d\alpha}$
0	0	0	0	0	0	0	0	0
0	6.09	6.01	0.425	6.10	0.429	5.93	0.419	6.01
0	21.83	20.87	0.233	21.83	0.234	21.63	0.238	20.88
20.26	47.45	46.24	0.150	47.45	0.151	47.36	0.148	46.24
33.01	66.34	60.68	0.163	66.46	0.166	67.15	0.172	60.73
57.10	80.83	76.15	0.152	80.90	0.154	81.24	0.163	76.20
70.36	91.90	93.87	0.129	91.83	0.132	91.02	0.138	93.91
104.63	125.76	120.92	0.127	125.72	0.128	125.15	0.120	121.10
119.35	127.12	123.28	0.121	127.17	0.124	126.68	0.125	123.30
130.61	148.98	125.10	0.096	148.98	0.096	148.83	0.128	124.84

$h_T^2 = D\sigma a^4 \hat{h}_T^2$, $\omega_\alpha^2 = D/(\sigma a^4)\hat{\omega}_\alpha^2$, $\lambda_\alpha^2 = D/(\sigma a^4)\hat{\lambda}_\alpha^2$, $\hat{\lambda}_\alpha = -\zeta_{d\alpha}\hat{\omega}_{d\alpha} \pm j(1-\zeta_{d\alpha}^2)^{1/2}\hat{\omega}_{d\alpha}$.

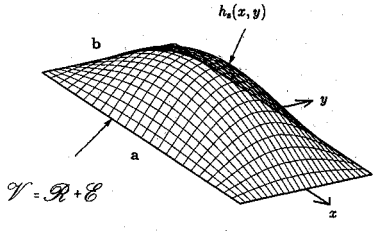

Fig. 2 Gyroelastic Purdue model for numerical example.

provided we interpret $\mathscr{H}$ and υ as follows:

$$\mathscr{H} \triangleq \text{row}\{\tfrac{1}{2}\nabla^\times \delta(\mathbf{r}-\mathbf{r}_i)\mathbf{h}_i^\times\}, \qquad \upsilon \triangleq \text{col}\{\beta_{xi}, \beta_{yi}, \beta_{zi}\}$$

wherein we have used the description [Eq. (8)] for $\mathbf{h}_s(\mathbf{r},t)$, and β_{xi}, β_{yi}, β_{zi} are the gimbal angles for gyro $\mathbf{h}_i$. Note that

$$U = R^{3n}, \qquad \langle \upsilon_1, \upsilon_2 \rangle_U = \upsilon_1^T \upsilon_2$$

In addition, the weighting operator $\mathscr{R}$ in this case is simply a matrix $\mathbf{R}$.

A time-invariant feedback law can be had by considering

$$\dot{\bar{\mathbf{P}}} \equiv \mathbf{O}, \qquad \bar{\mathbf{P}}\boldsymbol{\Omega} + \boldsymbol{\Omega}^T\bar{\mathbf{P}} + \tfrac{1}{4}\bar{\mathbf{P}}\boldsymbol{\Omega}^{-T}\mathbf{W}\boldsymbol{\Omega}^{-1}\bar{\mathbf{P}} - \mathbf{Q} = \mathbf{O} \quad (56)$$

which corresponds to the case of an infinite terminal time ($T \to \infty$) in Eqs. (45) and (46). If the rank of $\mathbf{W}$ is denoted by l, then $\mathbf{W}$ admits the representation $\bar{\mathbf{B}}\bar{\mathbf{B}}^T$, where $\bar{\mathbf{B}}$ has column dimension l. If $(\boldsymbol{\Omega}, \bar{\mathbf{B}})$ is controllable and $(\mathbf{Q}, \boldsymbol{\Omega})$ is observable, then the eigenvalues of $-[\boldsymbol{\Omega} + \frac{1}{4}\boldsymbol{\Omega}^{-T}\mathbf{W}\boldsymbol{\Omega}^{-1}\bar{\mathbf{P}}]$ have negative real parts.[12] Strictly speaking, these results hold only for the case of a finite number of mode pairs and no damping as the open-loop system is clearly asymptotically stable in the damped case. In the case of a finite terminal time, Lions[13] presents arguments suggesting that modal expansions for $\mathscr{P}$ will converge. Gibson[14] has examined the optimal control of elastic systems with infinite terminal time and pointwise force actuators (with and without damping).

V. Numerical Example

To illustrate some of our theoretical results, we consider the Purdue model,[15] which is an equivalent continuum representation of a typical large space structure. The structure consists of a uniform elastic plate of mass density σ (per unit area) and modulus of rigidity D. Located at the center of the plate is a rigid body, assumed to be of negligible physical size. Its inertial properties are summarized by

$$m_r = 0.1m_e, \qquad I_{rx} = 0.01I_{ex}, \qquad I_{ry} = 0.01I_{ey}$$

where

$$m_e = \sigma ab, \qquad I_{ex} = \sigma ab^3/12, \qquad I_{ey} = \sigma a^3 b/12$$

The aspect ratio and Poisson's ratio are $a/b = 2.5$ and $\nu = 0.30$, a and b being the dimensions of the plate. Since we shall consider only out-of-plane deflections, the displacement function is a scalar

$$w(x,y,t) = w_0 + \theta_x y - \theta_y x + u_e, \qquad (x,y) \in E$$

The stiffness operator is given by

$$\mathscr{K} = D\nabla^4$$

where ∇^4 is the biharmonic operator.

We endow the model with a distribution of gyricity directed normal to the plate surface and

$$h_s(x,y) = \frac{h_T \pi^2}{4ab} \cos\left(\frac{\pi x}{a}\right) \cos\left(\frac{\pi y}{b}\right) \quad (57)$$

where

$$h_T = \int\int_A h_s(x,y)\, dx\, dy$$

is the total gyricity (see Fig. 2). Modeling the gyricity distribution as a continuum is in keeping with the nature of the Purdue model. However, it will be instructive to compare results obtained using Eq. (57) with those obtained assuming a finite number of control moment gyros. Thus, we shall also consider a gyricity distribution

$$\tilde{h}_s = \sum_i h_i \delta(\mathbf{r} - \mathbf{r}_i) \quad (58)$$

equivalent to h_s in the following sense: The location of the wheels $\mathbf{r}_i$ and the magnitude of the wheel momenta h_i are determined by dividing the structure into an $n \times n$ grid of identical rectangles denoted by $\square_i$. Then we take

$$h_i \triangleq \int\int_{\square_i} h_s\, dx\, dy, \qquad i = 1,\ldots,n^2$$

and $\mathbf{r}_i$ as the centerpoint of the rectangle $\square_i$.

A finite-element procedure, employing 16 elements and 100 degrees of freedom, was used in the numerical analysis. For details consult Ref. 7. The first 10 frequencies for the elastic and gyroelastic cases are recorded in Table 1. The geometry of the gyricity distribution is such that the vehicle does not exhibit a pseudorigid mode. However, the two rigid-body

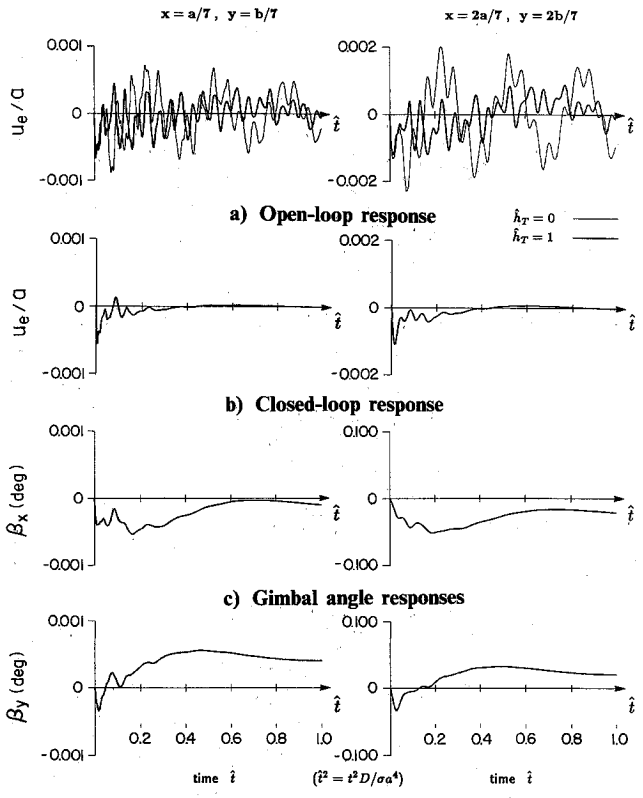

Fig. 3 Open- and closed-loop responses (continuous gyricity).

modes associated with rotation in the elastic case become a precessional mode.[4] The reader should compare the frequencies obtained with continuous gyricity with those calculated for an equivalent pointwise distribution ($n = 7$). Agreement is very good, supporting the concept of a continuous gyricity distribution as a model for a "cloud of wheels."

For the simulation results which follow, we assume quiescent initial conditions and an impulsive disturbance force located at the rigid body that could represent a thruster force such as that used in a stationkeeping maneuver. The magnitude of the impulse is such that

$$\int_{0-}^{0+} \iint_A f_t \delta(\mathbf{r},t)\, dx\, dy\, dt = 0.01\sqrt{D\sigma_a{}^2}$$

For damping we assume a constant damping ratio:

$$\zeta_\alpha \equiv 0.01, \qquad \alpha = 1,2,3,...$$

and neglect, as argued earlier, the eigenfunction perturbations. The elastic deflection (open-loop) of the plate in the elastic and gyroelastic cases for two points on the structure is displayed in Fig. 3a. The mere presence of gyricity is beneficial in "stabilizing" the shape of the structure. Indeed, the effect is progressively enhanced as the gyricity level is increased. This can be traced to the fact that gyricity causes a shift in energy to higher modes.[7]

Let us now return to the case of active control. For continuous gyricity, we consider the following performance index:

$$J = \frac{1}{2}\int_0^T \left\{ \iint_A [\sigma \dot{w}^2 + u_e D\nabla^4 u_e + r(\beta_x^2 + \beta_y^2)]\, dx\, dy - m^{-1}\left[\iint_A \sigma \dot{w}\, dx\, dy\right]^2 \right\} dt$$

where $\beta_x(x,y,t)$ and $\beta_y(x,y,t)$ are gimbal angles associated with the gyricity distribution and $m \triangleq m_r + m_e$. We have chosen $\mathscr{R} = r\mathbf{1}$ and

$$\mathscr{Q} = \begin{bmatrix} \sigma 1 - m^{-1}\sigma 1\rangle\langle \sigma 1 & \cdot \\ \cdot & D\nabla^4 \end{bmatrix}$$

according to Eq. (47). In the pointwise case, we make the change

$$\iint_A r(\beta_x^2 + \beta_y^2)\, dx\, dy \to \dot{\boldsymbol{\beta}}^T \mathbf{R} \dot{\boldsymbol{\beta}}$$

where

$$\dot{\boldsymbol{\beta}} = \text{col}\{\dot{\beta}_{x_i}, \dot{\beta}_{y_i}\}, \quad \mathbf{R} = \text{diag}\{rA_i, rA_i\}, \quad A_i = \iint_{\square_i} dx\, dy \equiv ab/n^2$$

We call attention to the determination of the matrix $\mathbf{W}$. The finite-element approximation of the mode shape $\boldsymbol{u}_\alpha$ can be written as

$$\boldsymbol{u}_\alpha \doteq \boldsymbol{\Delta}(x,y)\boldsymbol{q}_\alpha$$

where $\boldsymbol{\Delta}$ is a matrix of basis shape functions and $\boldsymbol{q}_\alpha$ is the eigencolumn obtained from the discretized eigenproblem. Hence, the elements of $\mathbf{W}$ can be written as

$$W_{\alpha\beta} = \boldsymbol{q}_\alpha^T \hat{\mathbf{W}} \boldsymbol{q}_\beta, \quad \hat{\mathbf{W}} = \iint_A (\mathscr{H}^* \boldsymbol{\Delta})^T \mathscr{R}^{-1} (\mathscr{H}^* \boldsymbol{\Delta})\, dx\, dy$$

In the present case, we can furthermore write the $\hat{\mathbf{W}}$ matrix as

$$\hat{\mathbf{W}} = r^{-1} \iint_V h_s^2(x,y) \left[\frac{\partial \boldsymbol{\Delta}^T}{\partial x}\frac{\partial \boldsymbol{\Delta}}{\partial x} + \frac{\partial \boldsymbol{\Delta}^T}{\partial y}\frac{\partial \boldsymbol{\Delta}}{\partial y} \right] dx\, dy$$

When considering pointwise gyros, this matrix can be calculated using

$$\hat{\mathbf{W}}^{(n)} = \sum_{i=1}^{n^2} (rA_i)^{-1} h_i^2 \left[\frac{\partial \boldsymbol{\Delta}^T}{\partial x}\frac{\partial \boldsymbol{\Delta}}{\partial x} + \frac{\partial \boldsymbol{\Delta}^T}{\partial y}\frac{\partial \boldsymbol{\Delta}}{\partial y} \right]_{r=r_i}$$

and given the way in which $\mathbf{R}$ and h_i are selected, $\hat{\mathbf{W}}^{(n)} \to \hat{\mathbf{W}}$ as $n \to \infty$. In fact, the continuum description of the gyricity distribution and associated control problem may be viewed as the limiting case of successive control problems involving n^2 gyros, with $n \to \infty$ and the total stored angular momentum h_T remaining constant.

The weighting constant is set at $r = 2\sigma a^2$. The choice of $\mathscr{Q}$ yields

$$\mathbf{Q} = \text{diag}\{2\omega_\alpha^2, 2\omega_\alpha^2\}$$

For purposes of this example, we have used the first 25 mode pairs in solving the Riccati equation. The first 10 closed-loop eigenvalues for both cases (h_s and $\tilde{h}_s$) are listed in Table 1. Once again the agreement between the two cases is quite good. Numerical experience indicates that the discrepancy is reduced as n is increased. It is interesting to note that the choice of performance index results in closed-loop damping ratios that tend to fall off with frequency (there are exceptions). Simulation results for the closed-loop case (continuous gyricity) appear in Figs. 3b–3d. The dynamic response is displayed at two points on the structure as are the gimbal angle histories. We omit the results for the case of pointwise gyricity since they are indistinguishable from the continuous case.

It is worthwhile noting that, if $\mathbf{Q}$ is block diagonal (as it is here), then $\bar{\mathbf{P}}$ is block diagonal if $\mathbf{W}$ is. Present numerical studies indicate that $\mathbf{W}$ is diagonally dominant and almost block diagonal. If we neglect the "off-diagonal" entries, then the solution of the algebraic Riccati equation [Eq. (56)] reduces to the solution of N 2×2 Riccati equations, providing significant computational savings. The closed-loop modal

system matrix is block diagonal as well. Employing this simplification yields the closed-loop eigenvalues shown in Table 1. Scanning these values, we see that there is little difference from that involving a complete solution of the Riccati equation. The approximation yields damping factors that are somewhat higher than those resulting from a full solution. The simulation results though were graphically identical. Meirovitch and Baruh[16] obtained 2×2 Riccati equations for lightly damped gyroelastic systems using the independent modal-space control technique. Their approach, however, employs uncoupled penalization of the modal coordinates and modal forces from the outset.

VI. Concluding Remarks

As is evident from the numerical example, an active gyricity distribution can be extremely effective in providing attitude and shape control for flexible spacecraft. It is also notable that a "passive" gyricity distribution, i.e., an open-loop configuration, can potentially be very beneficial for "shape stabilization." This use of gyricity represents, in essence, an extension of the notion of spin (or, to some, gyroscopic) stabilization for rigid spacecraft.

The continuum approach, used throughout the theoretical development, offers a very elegant formulation that allows us the fullest latitude for generalization (in particular, to consider distributed actuators). Moreover, with a mere reinterpretation of symbols, the results can be applied directly to discretized systems. It has also been numerically demonstrated that a continuous distribution of gyricity is a suitable and effective model for a distribution of control moment gyros over a structure.

The optimal control formulation proved very successful and straightforward to implement. A modal expansion was introduced for the Riccati operator $\mathscr{P}$, which takes into account rigid-body motion. The resulting discretized Riccati equation was shown to reduce to a set of bicoupled (2×2 matrix) Riccati equations. This simplification, however, was rendered possible by the diagonal dominance of the matrix involved in the nonlinear term. Although this is an empirical result for the chosen example, it should be worthwhile to explore its general application. The computational consequences are significant, since it greatly reduces the effort required to solve the Riccati equation and the closed-loop modal equations of motion furthermore retain their bicoupled form.

In conclusion, active gyric control appears to be an attractive method of controlling large flexible space structures. One can also look beyond the optimal control approach used here to consider decentralized control techniques and momentum wheels as well as control moment gyros. Finally, we add that there should exist potential advantages in using gyric control during slewing maneuvers of flexible spacecraft.

Appendix

Since the performance index [Eq. (46)] is (strictly) convex, a necessary and sufficient condition for optimality of $\upsilon^\star$ is[13]

$$\delta J(\upsilon^\star;\upsilon-\upsilon^\star) \triangleq \frac{\mathrm{d}}{\mathrm{d}\epsilon} J[\upsilon^\star+\epsilon(\upsilon-\upsilon^\star)]\bigg|_{\epsilon=0} \geq 0, \quad \forall \upsilon \in U_{ad} \quad \text{(A1)}$$

The above condition becomes

$$\frac{1}{2}\int_0^T \langle \chi(\upsilon^\star), 2\chi(\upsilon)-2\chi(\upsilon^\star)\rangle + \langle \upsilon^\star, \mathscr{R}\upsilon-\mathscr{R}\upsilon^\star\rangle_U \,\mathrm{d}t \geq 0, \quad \forall \upsilon \in U_{ad} \quad \text{(A2)}$$

where $\chi(\upsilon^\star)$ denotes the optimal trajectory. Introducing the adjoint equation

$$-\mathscr{E}\dot{\xi}(\upsilon^\star) + \mathscr{T}^*\xi(\upsilon^\star) = 2\chi(\upsilon^\star), \qquad \xi(\upsilon^\star)\big|_{t=T} = \mathbf{0} \quad \text{(A3)}$$

the left side of Eq. (A2) can be manipulated as follows:

$$\begin{aligned}
&\frac{1}{2}\int_0^T \langle -\mathscr{E}\dot{\xi}(\upsilon^\star) + \mathscr{T}^*\xi(\upsilon^\star), \chi(\upsilon)-\chi(\upsilon^\star)\rangle \\
&\quad + \langle \upsilon^\star, \mathscr{R}\upsilon-\mathscr{R}\upsilon^\star\rangle_U \mathrm{d}t \\
&= \frac{1}{2}\int_0^T \langle \xi(\upsilon^\star), \mathscr{E}\dot{\chi}(\upsilon) + \mathscr{T}\chi(\upsilon) - \mathscr{E}\dot{\chi}(\upsilon^\star) - \mathscr{T}\chi(\upsilon^\star)\rangle \\
&\quad + \langle \mathscr{R}\upsilon^\star, \upsilon-\upsilon^\star\rangle_U \,\mathrm{d}t \\
&= \frac{1}{2}\int_0^T \langle \xi(\upsilon^\star), \mathscr{B}\upsilon-\mathscr{B}\upsilon^\star\rangle + \langle \mathscr{R}\upsilon^\star, \upsilon-\upsilon^\star\rangle_U \,\mathrm{d}t \\
&= \frac{1}{2}\int_0^T \langle \mathscr{B}^*\xi(\upsilon^\star) + \mathscr{R}\upsilon^\star, \upsilon-\upsilon^\star\rangle_U \,\mathrm{d}t
\end{aligned}$$

Therefore, the optimality condition can be written as

$$\frac{1}{2}\int_0^T \langle \mathscr{B}^*\xi(\upsilon^\star) + \mathscr{R}\upsilon^\star, \upsilon-\upsilon^\star\rangle_U \,\mathrm{d}t \geq 0, \qquad \forall \upsilon \in U_{ad}$$

Since the optimal control is unique (owing to the strict convexity of J), our choice of admissible controls [Eq. (45)] yields

$$\upsilon^\star(r,t) = -\mathscr{R}^{-1}\mathscr{B}^*\xi(r,t) \quad \text{(A4)}$$

where

$$-\mathscr{E}\dot{\xi}(r,t) + \mathscr{T}^*\xi(r,t) = 2\chi(r,t), \qquad \xi(r,T) = \mathbf{0}$$

(The functional dependence on $\upsilon^\star$ has been dropped.) The state equation becomes

$$\mathscr{E}\dot{\chi} + \mathscr{T}\chi = -\mathscr{B}\mathscr{R}^{-1}\mathscr{B}^*\xi, \qquad \chi(r,0) = \chi_0$$

and the transformation $\xi(r,t) = \mathscr{P}(t)\mathscr{E}\chi(r,t)$ leads to the operator Riccati equation [Eq. (49)]. The optimal value of the performance index can be had by substituting Eqs. (A3) and (A4) into J:

$$\begin{aligned}
J(\upsilon^\star) &= \frac{1}{2}\int_0^T \langle \chi, -\mathscr{B}\dot{\xi} + \mathscr{T}^*\xi\rangle - \langle \upsilon, \mathscr{B}^*\xi\rangle_U \,\mathrm{d}t \\
&= \frac{1}{2}\int_0^T \langle \mathscr{E}\dot{\chi} + \mathscr{T}\chi, \xi\rangle - \langle \mathscr{B}\upsilon, \xi\rangle \,\mathrm{d}t - \frac{1}{2}\langle \chi(t), \mathscr{E}\xi(t)\rangle\Big|_{t=0}^{t=T} \\
&= \frac{1}{2}\langle \chi_0, \mathscr{E}\xi(r,0)\rangle \\
&= \frac{1}{2}\langle \chi_0, \mathscr{E}\mathscr{P}_0\mathscr{E}\chi_0\rangle
\end{aligned}$$

where $\mathscr{P}_0 \triangleq \mathscr{P}(0)$.

Acknowledgments

The authors would like to thank Ida Albert for the figures. This research has been funded by the Natural Sciences and Engineering Research Council of Canada.

References

[1]D'Eleuterio, G. M. T. and Hughes, P. C., "Dynamics of Gyroelastic Continua," *ASME Journal of Applied Mechanics*, Vol. 51, June 1984, pp. 412–422.

[2]D'Eleuterio, G. M. T., "Dynamics of Gyroelastic Vehicles," Ph.D. Dissertation, Institute for Aerospace Studies, University of Toronto, Downsview, Ontario, 1984; UTIAS Rept. 300, 1986.

[3]D'Eleuterio, G. M. T., "Dynamics of Gyroelastic Space Vehicles," Fifth VPI & SU/AIAA Symposium on Dynamics and Control of Large Structures, Blacksburg, VA, June 12–14, 1985.

[4]D'Eleuterio, G. M. T. and Hughes, P. C., "Dynamics of Gyroelastic Spacecraft," *Journal of Guidance, Control, and Dynamics*, Vol. 10,

July–Aug. 1987, pp. 401–405.
[5]Montgomery, R. C. and Sundararajan, N., "Identification of a Two-Dimensional Grid Structure using Least Square Lattice Filters," *Journal of Astronautical Science*, Vol. 33, No. 1, Jan–March, 1985, pp. 35–47.
[6]Özgüner, Ü., Yurkovich, S., Martin, J., II, and Al-Abbass, F., "Decentralized Control Experiments on NASA's Flexible Grid," *Proceedings of the 1986 American Control Conference*, Seattle, WA, June 18–20, 1986, pp. 1045–1051.
[7]Damaren, C. J., "An Optimal Control Formulation for Lightly Damped, Gyroelastic Continua," M.S. Thesis, Institute for Aerospace Studies, University of Toronto, Downsview, Ontario, 1987.
[8]Meirovitch, L. and Ryland, G., II, "Response of Slightly Damped Gyroscopic Systems," *Journal of Sound and Vibration*, Vol. 67, No. 1, 1979, pp. 1–19.
[9]Lim, K. B., Junkins, J. L., and Wang, B. P., "Re-examination of Eigenvector Derivatives," *Journal of Guidance, Control, and Dynamics*, Vol. 10, Nov.–Dec. 1987, pp. 581–587.
[10]Hughes, P. C., "Modeling of Energy Dissipation (Damping) in Flexible Space Structures," Dynacon, Downsview, Ontario, Rept. MSAT-6, March 1982 (DOC Contractor Rept. DOC-CR-SP-82-024).
[11]Kadison, R. V. and Ringrose, J. R., *Fundamentals of the Theory of Operator Algebras*, Academic, New York, 1983, Vol. I, Chap. 2.
[12]Damaren, C. J. and D'Eleuterio, G. M. T., "Controllability and Observabillity of Gyroelastic Systems" (to be published) 1989.
[13]Lions, J. L., *Optimal Control of Systems Governed by Partial Differential Equations*, Springer-Verlag, New York, 1971.
[14]Gibson, J. S., "An Analysis of Optimal Modal Regulation: Convergence and Stability," *SIAM Journal of Control Optimization*, Vol. 19, No. 5, Sept. 1981, pp. 686–707.
[15]Hablani, H. B., "Constrained and Unconstrained Modes: Some Modeling Aspects of Flexible Spacecraft," *Journal of Guidance and Control*, Vol. 5, March–April 1982, pp. 164–173.
[16]Meirovitch, L. and Baruh, H., "Optimal Control of Damped Flexible Gyroscopic Systems," *Journal of Guidance and Control*, Vol. 4, March–April 1981, pp. 157–163.